

We are IntechOpen, the world's leading publisher of Open Access books Built by scientists, for scientists

6,900

Open access books available

185,000

International authors and editors

200M

Downloads

Our authors are among the

154

Countries delivered to

TOP 1%

most cited scientists

12.2%

Contributors from top 500 universities



WEB OF SCIENCE™

Selection of our books indexed in the Book Citation Index
in Web of Science™ Core Collection (BKCI)

Interested in publishing with us?
Contact book.department@intechopen.com

Numbers displayed above are based on latest data collected.
For more information visit www.intechopen.com



Palm oil as Corrosion Inhibitor for Aluminium Car Radiator

Junaidah Jai

Additional information is available at the end of the chapter

<http://dx.doi.org/10.5772/57273>

1. Introduction

Organic compounds are found to be effective corrosion inhibitors due to the adsorption of molecules and ions on the metal surface. As reviewed by Maayta and Al-Rawashdeh [1], the extent of adsorption of an inhibitor depends on many factors such as the nature of the surface charge of the metal, the mode of the adsorption of the inhibitor, the inhibitor's chemical structure and the type of the corrosive solution. The presence of large molecules with functional groups containing heteroatoms (such as oxygen, nitrogen, sulphur, phosphorus), triple bonds or aromatic rings in the inhibitor's chemical structure enhances the adsorption process [2]. There has been a growing trend on the use of natural resources as corrosion inhibitors, which are environmentally friendly, cheap and readily available. Table 1 lists out some works done to evaluate various natural resources as corrosion inhibitors.

Generally, not many works have been done on the application of natural oils as corrosion inhibitors. One of the common and abundant natural oils in Asian countries is palm oil. Crude palm oil (CPO) contains equal amounts of saturated and unsaturated fatty acids which are palm stearin and palm olein, respectively. Palm olein contains monounsaturated and polyunsaturated acids consisting of oleic and linoleic acids. Both oleic and linoleic acids contain carbonyl groups which gives palm olein the potential to act as a corrosion inhibitor.

Currently, due to its lightweight property and corrosion resistance, Al alloy is used to replace copper as the material for car radiators. Numerous methods have been applied to protect Al against corrosion. One of the attempts is to use palm olein as an environmentally friendly corrosion inhibitor. However little or no work on this matter has been reported. Therefore, this work focuses on the effect of palm olein as a corrosion inhibitor for Al which would be suitable for application in Al car radiators.

Natural resources	References
natural honey	El-Etre & Abdallah, 2000 [3]
Vanillin	El-Etre, 2001 [4]
<i>opuntia ficus mill</i> (family of cactaceae)	El-Etre, 2003 [5]
<i>nypa fruticans wurmb</i>	Orubite & Oforka, 2004 [6]
lawsonia (henna) extract	El-Etre, Abdallah, & El-Tantawy, 2005 [7]
olive leaves	El-Etre, 2007 [2]
fenugreek leaves	Noor, 2007 [8]
<i>musa sapientum</i> peels	Eddy & Ebenso, 2008 [9]
pennyroyal oil from <i>mentha pulegium</i>	Bouyanzer et al., 2006 [10]
artemisia oil	Benabdelah, Benkaddour, & Hammouti, 2006 [11]
	Ouachikh et al., 2009 [12]
	Kalaiselvi et al., 2010 [13]
	Bammou et al., 2011 [14]
	Garai et al., 2012 [15]
	Huang et al., 2013 [16]
fennel seed	Fouda et al., 2013 [17]

Table 1. Natural resources as corrosion inhibitor

2. Materials

Aluminium alloy (Al 6061) sheet with the composition listed in Table 2 was used. Its composition was determined by X-ray Fluorescence (XRF). Al 6061 was utilized in this work as it is a commonly used alloy in manufacturing automobiles, particularly used as the main material for car radiators.

Element	Si	Fe	Cu	Mn	Mg	Cr	Zn	Ti	Al
% (w/w)	0.549	0.269	0.205	0.004	6.240	0.118	0.008	0.008	92.599

Table 2. Chemical composition of aluminium alloy (Al 6061)

Palm oil is abundant in Malaysia and its new application has to be explored. Crude palm oil (CPO) contains equal amounts of saturated and unsaturated fatty acids which are palm stearin and palm olein, respectively. Palm olein (PO) can be separated from palm stearin by centrifuging. Composition of the PO is stated in Table 3, as determined through Gas Chromatograph/Mass Spectroscopy (GCMS) (Agilent Technologies 6890N). The main components of palm olein are oleic acids ($C_{18}H_{34}O_2$), hexadecanoic acid ($C_{16}H_{32}O_2$) and stigmasterol ($C_{29}H_{48}O$). The

minor components are nonadecene, octadecanoic acid, tetracosahexaene, campesterol, cyclopentane, tricosene and cyclooctacosanetetrona.

Components	Composition (%)
Oleic acid	18.10
Hexadecanoic acid	15.72
Stigmasterol	11.01
Nonadecene	9.74
Octadecanoic acid, methyl ester	6.34
Tetracosahexaene	2.15
Campesterol	1.46
Cyclopentane	0.73
Tricosene	0.35
Cyclooctacosanetetrona	0.33
Free fatty acid	34.00

Table 3. Composition of palm olein from crude palm oil

All fatty acids listed in Table 3 have a carboxylic group in their molecular structure. However, they are differentiated by the presence of other functional groups, such as single double bond in oleic acid and aromatic hydroxyl group in stigmasterol (Table 4).

Different types of additives can be used to enhance inhibition efficiency of any corrosion inhibitor. In this work, poly(oxyethylene)x-sorbitane-monolaurate commercially known as Tween 20 (T20), hexane and diethylene triamine (DETA) were used for this purpose.

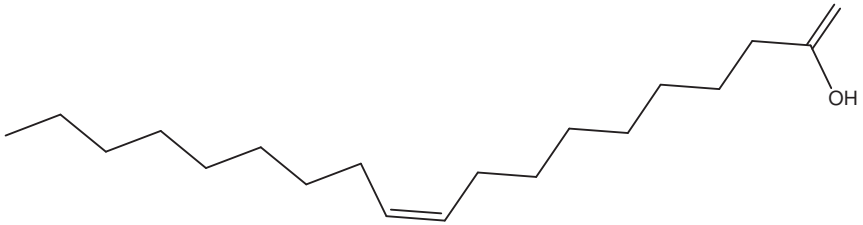
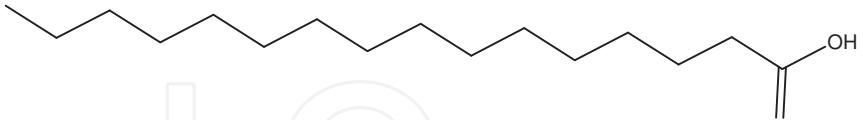
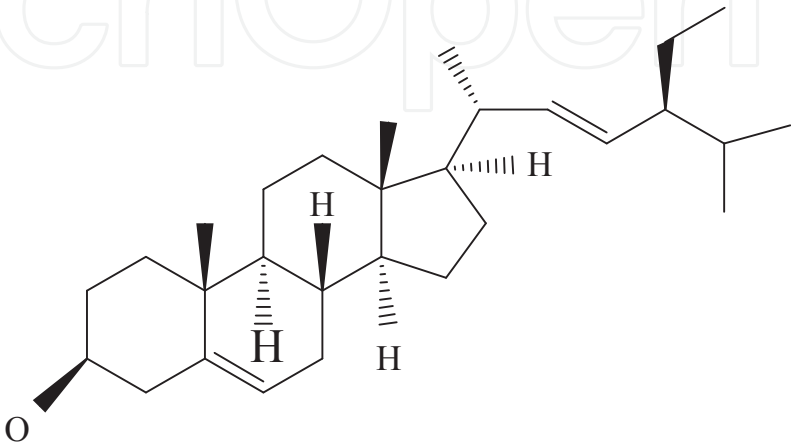
3. Formulation of corrosion inhibitor

Corrosion inhibitor should be formulated to suit the condition where it would be placed. For car radiators, the formulated corrosion inhibitor should be soluble in the coolant, thermally stable and effective within the range of the radiator's working pressure and temperature. In this work, the presence of an emulsifier, such as Tween 20, and a stabilizing agent, such as hexane, in the formulation is important, as palm olein is inherently unsoluble in water. Furthermore, the solubility and stability of the formulated corrosion inhibitor should be investigated by testing the corrosion inhibitor at different pH and temperatures since both factors give significant influence to the formulation. Diethylene triamine (DETA) was used to enhance the inhibition efficiency (IE) of the inhibitor at elevated temperatures.

Blends of palm olein and water in the presence of emulsifier and stabilizing agents at certain pH and temperature can produce stable emulsions with two separate layers; thick and dilute emulsions. Only the soluble and stable emulsion can be taken as the palm olein (PO) inhibitor. The solubility of an emulsion is considered good if there is no oily layer formed, whereas the stability of an emulsion is considered good if there is no oily layer formed after a prolonged period of time.

Analyses on the formulated PO inhibitor's concentration, pH, as well as micelle size and shape are very important since the inhibition and adsorption mechanism of the inhibitor on the aluminium surface can be predicted and understood from them.

Molar concentration of the PO corrosion inhibitor can be determined through acid-base titration method. The shape of micelles in the formulated PO corrosion inhibitor can be observed under optical microscopy (Axioskop 40, Zeiss) at 100 x magnification. As for the micelles size, it can be measured using particle size analyzer (Malvern Instrument, Mastersizer 2000).

Components	Molecular structures
Oleic acid	
Hexadecanoic acid	
Stigmasterol	

Components	Molecular structures
Cyclooctacosanetetrone	
Cyclopentane	
Nonadecene	
Octadecanoic acid	
Tetracosahexaene	
Tricosene	

Table 4. Molecular structures of the components in palm olein [18]

4. Corrosion study

Performance of the formulated inhibitor should be evaluated by several corrosion tests such as weight loss, potentiodynamic polarization and electrochemical impedance spectroscopy. For corrosion tests, 1 M HCl solution is commonly used as the corrosive media especially for aluminium alloy since it is easily attacked by Cl⁻ ions. In order to study the inhibition efficiency and inhibiting behaviour of the formulated corrosion inhibitor, metal has to be exposed to the corrosive media in the absence and presence of the inhibitor at different temperatures and concentrations of inhibitor. The chosen temperature range of the testing has to be based on the application of the inhibitor.

4.1. Weight loss (WL) study

Cleaned metal sheet with desired dimensions of 2 cm x 3 cm x 0.3 cm are used as test plates. Dimension and weight of the plate should be accurately measured prior to exposing the plate in a corrosive solution. The cleaned plate has to be suspended in the corrosive solution for several hours according to the desired exposure time. The plates were collected and retrieved at intervals of 1, 3, 6, 12, 24 and 48 hours for data collection. The collected plates should be

cleaned before the plate was weighed. The metal sample preparation and cleaning techniques are according to ASTM G1-90 [19]. Each experiment should be triplicated for significant result. Corrosion rate can be determined from the weight loss data using the following formula [20];

$$\text{Corrosion rate (millimeter per year)} = 87.6 \frac{W}{DAT} \quad (1)$$

where W is the weight loss (mg), D is the density of the Al sample (g/cm^3), A is the area of sample (cm^2) and T is the exposure time (h). The percentage of inhibition efficiency IE% for the weight loss method was calculated as follows;

$$IE\% = \left(\frac{W^0 - W}{W^0} \right) \times 100 \quad (2)$$

where W and W^0 are the weight loss of the Al 6061 with and without the inhibitor, respectively.

4.2. Potentiodynamic polarization (PP) study

Sample preparation is very important in corrosion studies. For PP test, the sample should be prepared as in Figure 1. Normally the metal sheet has to be cut into sample pieces having dimensions such as 1 cm x 1 cm x 0.03 cm. A copper wire has to be attached to one side of the flat surface of the sample for electrical connection before the samples are cold mounted in a blend of resin and hardener. Normally only 1 cm^2 surface area is exposed to the corrosive media. This surface should be mechanically polished with sandpaper grade of 180 followed by 600. The polished surface has to be cleaned with distilled water followed by acetone and finally dried.

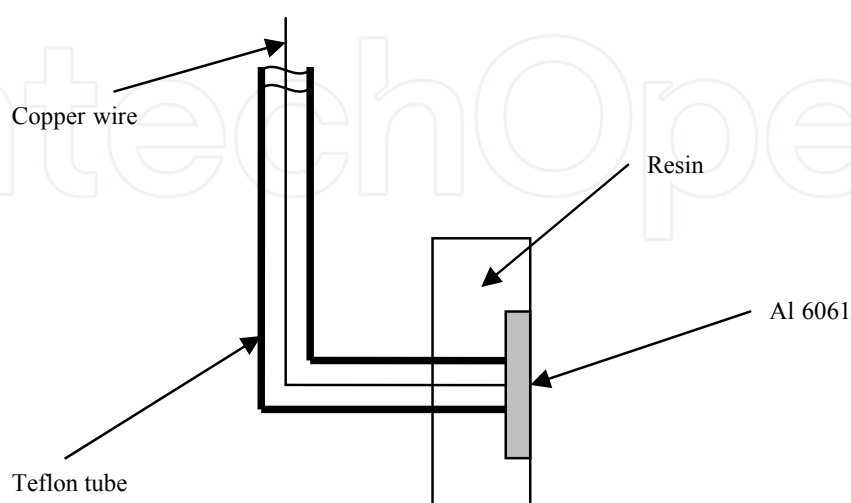


Figure 1. Sample assembly for potentiodynamic polarization measurement

Polarization measurement is carried out in a three-electrode electrochemical cell with consists of counter, working and reference electrodes. Normally, platinum mesh of 2 cm² and saturated calomel electrode (SCE) are used as the counter electrode and reference electrode, respectively, while the metal sample acts as the working electrode. An electrochemical station such as Voltalab (PGP201) apparatus can be used as a potential source. Figure 2 shows a schematic diagram of the electrochemical cell for the polarization test. Prior to measurement, the electrode is immersed in the test solution for 60 minutes at an open circuit condition until a steady state condition is achieved. Subsequently, PP measurements are taken at a scanning rate of 1 mV/s. For aluminium samples, the common potential range starts from -1200 to +200 mV versus the SCE.

For the PP study, corrosion behaviour of the sample has to be analyzed using corrosion potential (E_{corr}), corrosion current density (i_{corr}), polarization resistance (R_p), anodic Tafel slope (β_a), cathodic Tafel slope (β_c) and corrosion rate (CR). The IE for the PP study method can be calculated as follows;

$$IE\% = \left(\frac{i_{\text{corr}}^0 - i_{\text{corr}}}{i_{\text{corr}}^0} \right) \times 100 \quad (3)$$

where i_{corr} and i_{corr}^0 are the corrosion current density of the Al 6061 in the presence and absence inhibitor, respectively. Every experiment was repeated several times to make sure its reproducibility and the best are reported here.

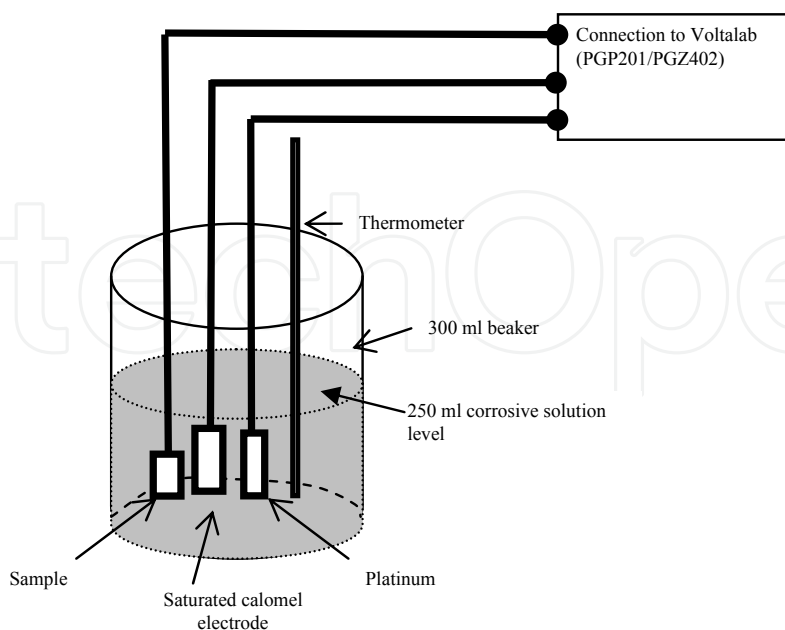


Figure 2. Schematic diagram of the electrochemical cell for polarization and electrochemical impedance spectroscopy tests

4.3. Electrochemical impedance spectroscopic (EIS) study

Sample preparation and EIS measurement are similar to that of the PP study. The EIS measurements were performed using AC signals of amplitude 10 mV peak to peak at the open circuit potential in the frequency range of 100 kHz to 100 mHz. Nyquist diagram can be determined from the experiment and the inhibition mechanism of the inhibitor can be explained from the calculated inductance or capacitance signals. The experiment should be repeated several times to make sure its reproducibility.

In confirming the corrosion behaviour of the inhibitor from corrosion tests, surface corrosion analysis using scanning electron microscope (SEM) should be done on the corroded surfaces. Performance test of the formulated inhibitor as anticorrosion for car radiator should also be done. As coolant and anticorrosion for car radiator, 95 wt% of coolant (glycerin) and the balance 5 wt% being the formulated inhibitor can be used.

5. Palm olein as anticorrosion for aluminium car radiator

5.1. Formulation of palm olein corrosion inhibitor

In formulating the PO inhibitor, emulsifier was added to enhance the solubility of palm olein in water. Figure 3 shows the corrosion rate of Al 6061 immersed in 1 M HCl solution containing different weight ratios of PO to T20 which were 5:0.5, 5:1.0 and 5:1.5. Within 1 to 6 hours of immersion time, the corrosion rates of all solution ratios were almost constant and similar to each other. Nevertheless, the 5:1.0 had shown the lowest corrosion rate followed by the 5:1.5 and 5:0.5 ratio solutions. A further increase in the immersion time from 6 to 24 hours had shown sharp increase in the corrosion rates for all ratios, with the 5:1.0 being the lowest followed by the 5:1.5 and 5:0.5. However, an increase in the immersion time from 24 to 48 hours had shown gradual reduction in the corrosion rate for all ratios. The results showed that despite the different weight ratios of PO to T20, all solutions produced almost similar corrosion rates. However, the solution with 5:1 ratio produced slightly lower corrosion rates than the other two solutions. The 5:1 ratio solution might have had reached its critical micelle concentration (CMC), upon which a further increase in the amount of emulsifier would not change or increase the corrosion rate, as explained by Al-Rawashdeh, and Mayata [21]. Thus, the POT20 stock solution with the weight ratio of PO to T20 as 5:1 was selected and subsequently used in this work.

The initial pH of 25% (v/v) POT20 in water was 4.5. Table 5 shows the effect of pH on the solubility of 25% (v/v) POT20 in distilled water. After 1 hour, the solution settles into two separate layers; an oily layer at the top and another dilute layer of emulsion at the bottom. The same finding was recorded for pH 5 and 11 solutions. Two separate layers indicated that PO was not fully soluble in water. On the other hand, three separate layers were observed for pH 7 solution; an oily layer at the top, a thick emulsion in the middle and a dilute emulsion at the bottom. After 24 hours, it was observed that pH 7 solution had the thinnest oily later. This finding suggested that at pH 7, the solubility of the PO in water had improved due to the better stability and smaller micelle size of the produced emulsion [22]. Therefore the pH 7 solution was used in the preparation of the formulation. However, the stability of the solution was still low. Table 6 shows the effect of temperature on the solubility and stability of the 25% (v/v)

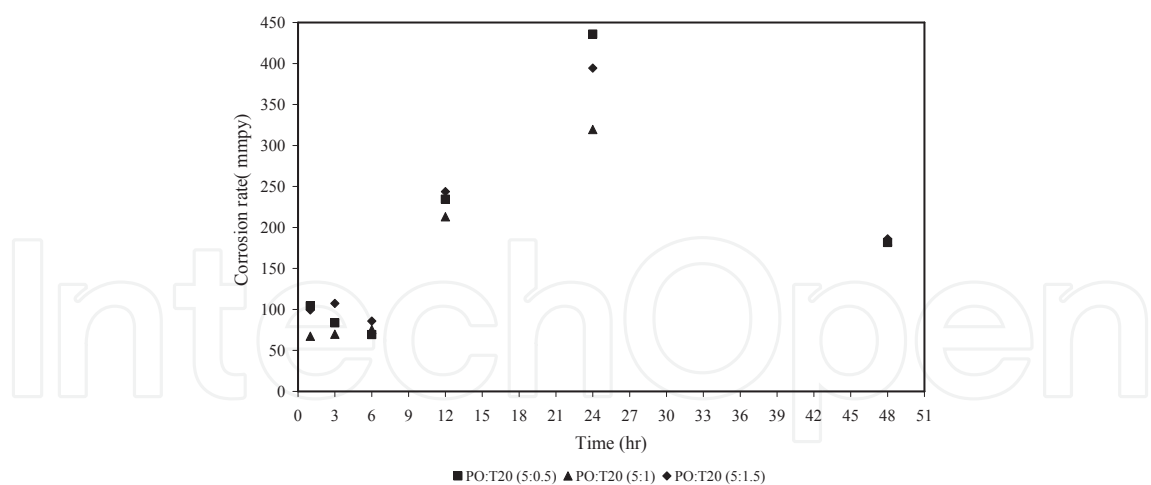


Figure 3. Corrosion rate of Al 6061 immersed in 1 M HCl with different weight ratio of PO to T20 at room temperature from weight loss test

POT20 in water. After one hour of settling down at 299 K, the three layers were observed. Similarly, an oily layer appeared at the top, a thick emulsion in the middle and a dilute emulsion at the bottom. However, at 323 K, two separate layers were observed with thick emulsion at the top and dilute emulsion at the bottom and no oily layer. The absence of an oily layer suggested that at 323 K, two forms of emulsions at formed; thick and dilute emulsions as agreed by Goyal, and Aswal [23]. In other words, the solubility of PO in water at 323K is higher than it is at 299 K. However, the stability of the solution at this temperature was still not satisfactory since after 24 hours of settling down, three separate layers were observed at both temperatures. Nevertheless, the 323 K was taken as the working temperature in the preparation of the formulation with some additives added to stabilize the formulation.

POT20, % (v/v)	25	25	25
Distilled water, % (v/v)	75	75	75
pH of the solution	pH 11	pH 7	pH 5
After 1 hour	Two separated layers observed; oily layer at the top and dilute emulsion at the bottom.	Three separated layers observed; oily layer at the top, thick emulsion in the middle and dilute emulsion at the bottom.	Two separated layers observed; oily layer at the top and dilute emulsion at the bottom.
After 24 hours			
Oil, % (v/v)	24	10	23
Thick emulsion, % (v/v)	0	14	0
Dilute emulsion, % (v/v)	76	76	77

Table 5. The effect of pH on the solubility and stability of POT20 in water

POT20, % (v/v)	25	25
Distilled water, % (v/v)	75	75
pH of the solution	pH 7	pH 7
Temperature	323 K	299 K
After 1 hour	Two separated layers were observed, thick emulsion at the top and dilute emulsion at the bottom	
After 24 hours	Three separated layers were observed, oily layer at the top, thick emulsion at the middle and dilute emulsion at the bottom.	
Oil, % (v/v)	4	6
Thick emulsion, % (v/v)	22	22
Dilute emulsion, % (v/v)	74	72

Table 6. The effect of temperature on the solubility of POT20 in water

Table 7 shows the effect of different concentrations of hexane varying at 5, 3, 1, 0.5 to 0%, (v/v) on the stability of 25% (v/v) POT20 in distilled water. The stability of the PO in water with 5, 3 and 1% (v/v) hexane remained unchanged until 9 days whilst with 0.5% (v/v), lasted for 14 days. The solution without hexane showed 12 days stability which was better than those in 5, 3 and 1% (v/v) hexane. This finding showed that the saturation concentration had been reached at above 1% (v/v) hexane; whereby further increase in hexane concentration did not improve the stability of the emulsion. Therefore, the optimum suitable volume ratio of hexane to POT20 was 0.5 to 25. Thus, this volume ratio was used in this work.

POT20, % (v/v)	25	25	25	25	25
Hexane, % (v/v)	5	3	1	0.5	0
Distilled water, % (v/v)	70	70	70	70	70
Stability, days	9	9	9	14	12

Table 7. Different amount of hexane on the stability of PO in water

The solubility and stability study revealed that the formulated PO inhibitor consists of two types of emulsion; thick emulsion and dilute emulsion. Dilute emulsion was soluble and stable in water, whereas the thick emulsion was insoluble in water. As such, the dilute emulsion was used as the corrosion inhibitor in this work and was labeled as POT20H. The thick emulsion was kept for future work.

5.2. Inhibition Efficiency (IE) of the palm olein corrosion inhibitor

Table 8 shows the IE of different concentrations of POT20H in 1 M HCl solution at 299 K as determined from the WL test. It was evident from the data that IE was directly proportional to POT20H concentration, but inversely proportional to immersion time. It increased with POT20H concentration from 10% (v/v) to 50% (v/v) but decreased with the increase of immersion time. Furthermore, IE of 50% (v/v) POT20H had remained 100% even after 48 hours of immersion time. In summary, at 299 K, 50% (v/v) POT20H consistently recorded better IE than any other concentration despite increasing immersion time from 1 to 48 hours.

Table 9 shows the IE of 50% (v/v) POT20H in 1 M HCl solution at different temperatures, 299, 323 and 343 K. Evidently, an increase in temperature reduced the IE of the inhibitor. POT20H seemed to perform the best at 299 K. In order to enhance POT20H's IE elevated temperatures, DETA was added in the formulation.

POT20H, % (v/v)	50	40	30	20	10
1 M HCl, % (v/v)	50	60	70	80	90
Immersion time (h)	Inhibition efficiency (%)				
1	100	97	95	94	83
3	100	99	99	99	96
6	100	99	95	94	91
12	100	94	86	71	68
24	100	84	60	34	22
48	100	56	36	13	6

Table 8. Inhibition efficiency of different concentrations of POT20H at 299 K from weight loss test

POT20H	50% (v/v)		
1 M HCl	50% (v/v)		
Immersion time (h)	Inhibition efficiency (%)		
	299 K	323 K	343 K
1	100	97	64
3	100	91	36
6	100	82	10
12	100	68	6
24	100	60	4
48	100	54	1

Table 9. Inhibition efficiency of POT20H solution at different temperatures from weight loss test

Figure 4 shows the corrosion rate determined from the WL test of Al 6061 in 1 M HCl and 50% (v/v) POT20H at 323 K with different concentrations of DETA. An addition of 3% (v/v) DETA into the 50% (v/v) POT20H solution remarkably reduced the corrosion rate as compared to that of the control 50% (v/v) POT20H. The corrosion rate of the control 3% (v/v) DETA was slightly higher than that of the 50% (v/v) POT20H with 3% (v/v) DETA solution which confirmed that inhibition was not solely due to DETA but the combination of POT20H and DETA. Reduction in the concentration of DETA from 3 to 2% (v/v) slightly reduced the corrosion rate. However, further reduction in the concentration from 2% (v/v) to 1% (v/v) followed by 0.5% (v/v) had markedly increased the corrosion rate. In other words, 50% (v/v) POT20H containing 2% (v/v) DETA showed the best IE. Consequently, for this study the best volume ratio of POT20H to DETA was 50 to 2 and this formulation was labeled as POT20HA.

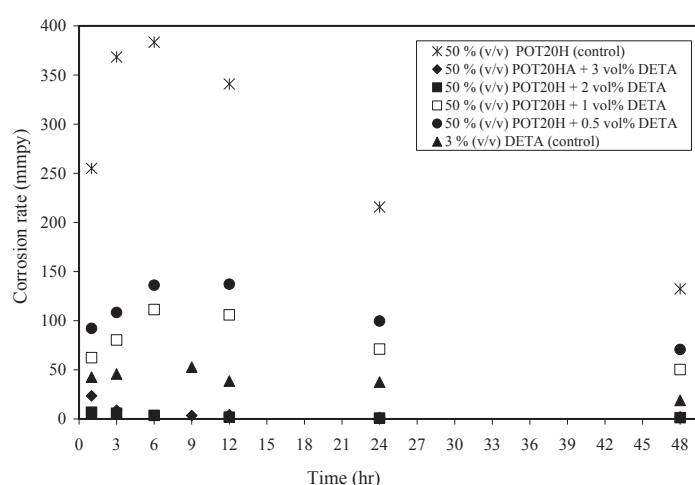


Figure 4. Corrosion rate from weight loss test of Al 6061 immersed in 1 M HCl and 50% (v/v) POT20H with the presence and absence of DETA at 323 K

5.3. Analysis of the palm olein corrosion inhibitor

The acid-base titration method was used to determine the molar concentration of the POT20HA. The initial pH of 30% (v/v) POT20HA in distilled water was 12.5 pH and 0.1 M HCl solution was used to neutralize the POT20HA. To calculate the molar concentration of the POT20HA the following reaction was considered; whereby 1 mol of POT20HA reacted with 1 mol of HCl [18],



Hence, in 30% (v/v) POT20HA, 0.1 M POT20HA reacted with 0.1 M of HCl. Table 10 shows the concentration of POT20HA which was extrapolated from the titration result.

Density of POT20HA was 0.98 g/cm³, as calculated from its weight and volume. From its concentration and density, the molar mass of POT20HA was calculated as 2969.70 g/mol. A

thin film of POT20HA was scanned under XRD at the phase angle of 10 to 70 degree. However, only one significant peak was observed, specifically at the phase angle of 2 to 5 degree. The XRD spectrum predicted that POT20HA contains n-phenyl-n-dodecanamide ($C_{18}H_{29}NO$) (illustrated in Figures 5). The compound reveals the presence of CON functional group, thus, it is classified as the amide family. The amide was synthesized from the reaction of carboxylic acid with an amine involving condensation process. Figure 6 shows the general reaction between a carboxylic acid and an amine to form an amide. Solubility of amide in water was almost similar to the solubility of ester in water; this explains POT20HA's slight solubility in water.

% (v/v)	Molarity (M)
10	0.03
20	0.07
30	0.10
40	0.13
50	0.17
100	0.33

Table 10. Concentrations of POT20HA

Optical microscopy reveals the solubility of POT20HA in water as shown in Figure 7. Particles with almost spherical in shape were observed in the emulsion, confirming the presence of micelles. The result shows that POT20HA is soluble in water in the form of micelles. Particles size of the micelles were distributed in 4 ranges, 0.04 to 0.6, 0.7 to 8, 9 to 50 and 60 to 300 μm . Less than 50% of the particles were 2.12 μm in size as presented in Figure 8.

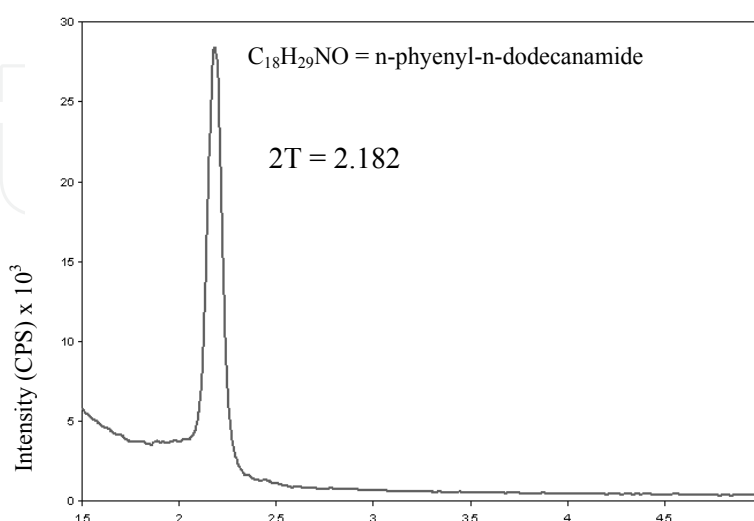


Figure 5. The XRD spectrum of POT20HA

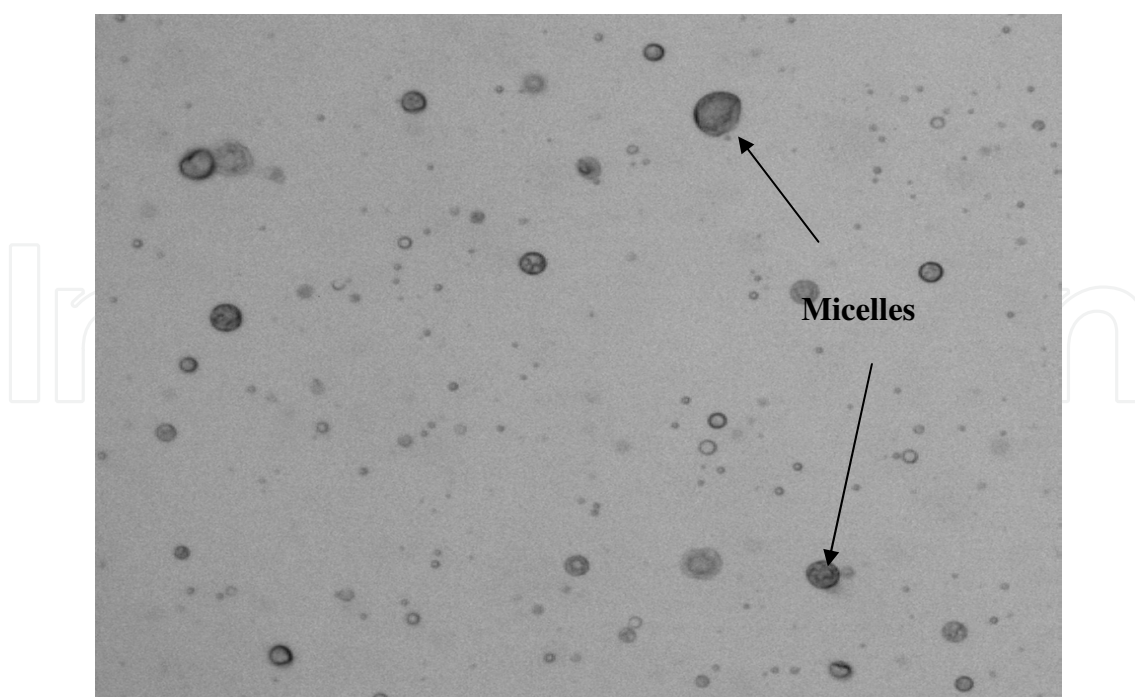


Figure 7. Optical microscopy observation on the POT20HA (100 x magnification)

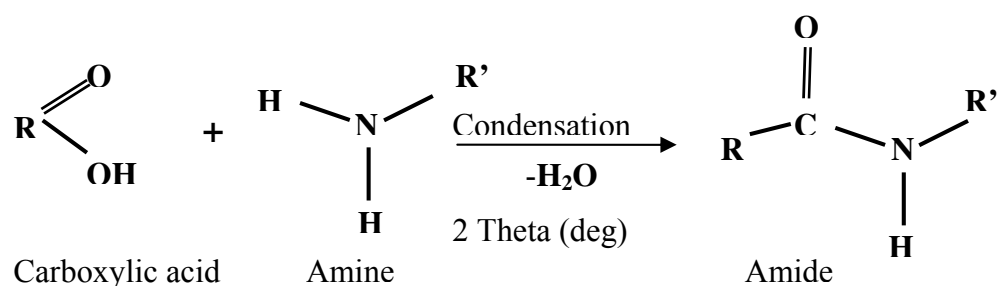


Figure 6. General reaction of carboxylic acid and amine to produce amide

Results had shown that T20 was a suitable emulsifier for PO in water with the weight ratio of PO to T20 set at 5:1. Hence the formulation is labeled as POT20. Besides, hexane had shown to be an excellent stabilizing agent with the volume ratio of hexane to POT20 set at 0.5:25. Consequently, solution with pH 7 and temperature of 323 K were found to be the most suitable condition in the preparation of the formulation. The mixture stirring speed was 125 rpm for the duration of 1 hour. As mentioned earlier, the formulation produced two emulsions i.e. dilute and thick emulsions. The dilute emulsion known as POT20H was used as the PO inhibitor due to its solubility in water. In enhancing the IE of the POT20H at elevated temperature, DETA was added in the formulation and the volume ratio of POT20H to DETA was 50:2 and was labelled as POT20HA. The POT20HA was chosen as the PO corrosion inhibitor in this study. As predicted, POT20HA consists of n-phenyl-n-dodecanamide compound which is the

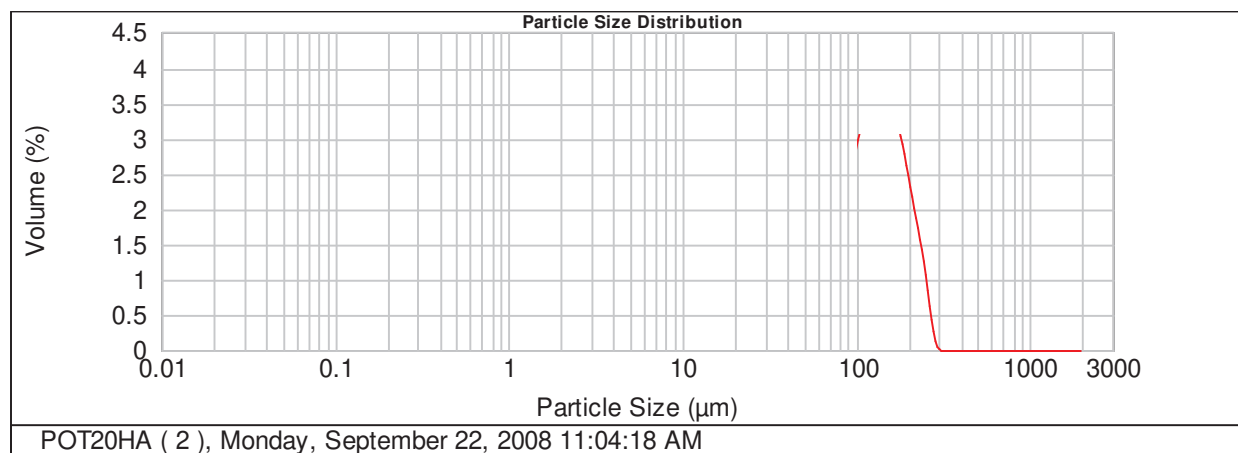


Figure 8. Distributions of POT20HA micelles size

family of amide and exists in the form of spherical micelle. The Inhibition behaviour of POT20HA was subsequently investigated through corrosion tests.

5.4. Corrosion evaluation

They are several corrosion test techniques which can be used to study the inhibition behaviour of an inhibitor. However, the most common methods used are weight loss, potentiodynamic polarization as well as electrochemical impedance spectroscopy.

5.4.1. Weight loss measurement

Figure 9 shows the corrosion rates of Al 6061 in 1 M HCl solution in the presence of POT20HA at 299 K. The corrosion rate of Al 6061 was very much higher in the absence of POT20HA as compared to the corrosion rates measured in the presence of varying levels of POT20HA. Corrosion occurred due to the presence of water, air, Cl^- and H^+ , which accelerated the corrosion process of the Al [20]. Increasing immersion time from initial to 3 hours significantly increased the corrosion rate. On the hand, further increase in the immersion time from 6 to 12 and 24 hours resulted in decrease in the corrosion rate. After 24 hours, the corrosion rate had reached its steady state. The same corrosion rate behaviour was obtained by Radzi [24] when Zn-Al coated low carbon steel wires were fully immersed in 3.5% NaCl solution. Nevertheless, increasing the immersion time from 3 to 48 hours reduced the corrosion rate by 78%. The reduction was due to the presence of aluminium hydroxide, which covered the Al 6061 surface [25].

The observed reduction in corrosion rates of Al 6061 in response to the increase of POT20HA concentrations indicated the positive effect of the inhibitor, as shown in Figure 9(b). Test solutions containing 0.03 and 0.07 M POT20HA showed similar corrosion behaviour, whereby a reduction in the corrosion rate was observed for the first three hours of immersion. This shows the ability of POT20HA to form a protective layer on the Al 6061 surface. However, an increase in the immersion time from 3 to 6 and 12 hours had shown slight increase and reduction in the corrosion rate, respectively.

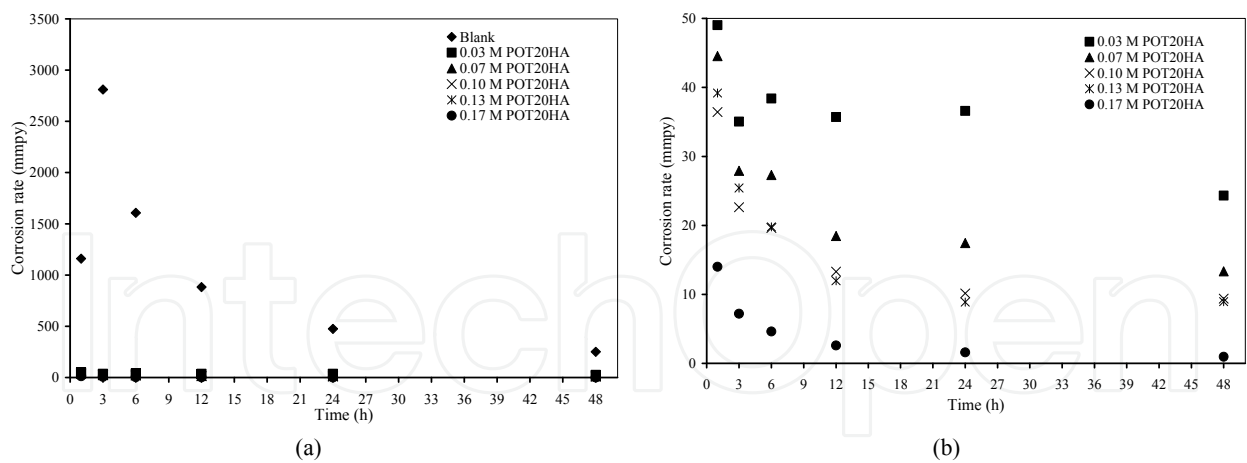


Figure 9. Corrosion rate of Al 6061 in 1 M HCl solution (a) with and without the presence of POT20HA and (b) with different concentrations of POT20HA at 299 K

Subsequently, after 24 hours, there was a small decrease in the corrosion rate of Al 6061 in the 0.07 M POT20HA but a slight increase in the 0.03 M. The increase and decrease of the corrosion rate suggested that there was insufficient surface coverage by the POT20HA on the Al 6061 surface. Diffusion of chloride ions (Cl^-) and hydrogen ions (H^+) through the pores of the uncovered surface led to the dissolution of Al [26, 27]. Consequently, the Al dissolution eventually led to the formation of corrosion product which repassivated the Al surface, which in turn reduced the corrosion rate. Tests on 0.10, 0.13 and 0.17 M POT20HA showed a direct reduction in corrosion rates from initial to 24 hours of immersion time. Eventually after 24 hours, the corrosion rate leveled as it reached its steady state. Therefore, it was evident that 0.10, 0.13 and 0.17 M POT20HA had produced excellent surface coverage which was not easily penetrated by Cl^- ions. In other words, 0.10, 0.13 and 0.17 M POT20HA produced better surface coverage than 0.03 and 0.07M POT20HA.

The corrosion rates of Al 6061 immersed in different concentrations of POT20HA at 323 and 343 K are shown in Figures 10 (a) and (b), respectively. Corrosion behaviour of Al 6061 was almost similar at both temperatures. For every concentration at both temperatures, an increase in the immersion time from initial to 24 hours had shown continuous gradual decrease in the corrosion rate. In each case, corrosion rate reached its steady state after 24 hours. In summary, 0.17 M POT20HA showed the lowest corrosion rate at both temperatures under study.

Table 11 reveals the IE of different concentrations of POT20HA at different temperatures. The IE increased with increasing concentration of POT20HA at 299, 323 and 343 K. However, the IE decreased with increasing temperature. At all temperatures and concentrations under study, an increase in the immersion time from initial to 3 hours had shown gradual increase in the IE. On the other hand, further increase in the immersion time from 3 to 24 hours had shown reduction in the IE. Nevertheless, IE of POT20HA at 299 K was the highest followed by those at 323 and 343 K. The IE was considered excellent when the value was equal or higher than 95%. The 0.07, 0.10, 0.13 and 0.17 M POT20HA at 299 K had shown excellent IE. On the other hand, at higher temperatures of 323 and 343 K, only 0.17 M POT20HA showed excellent IE. In general, the 0.17 M POT20HA had exhibited excellent IE at all temperatures under study.

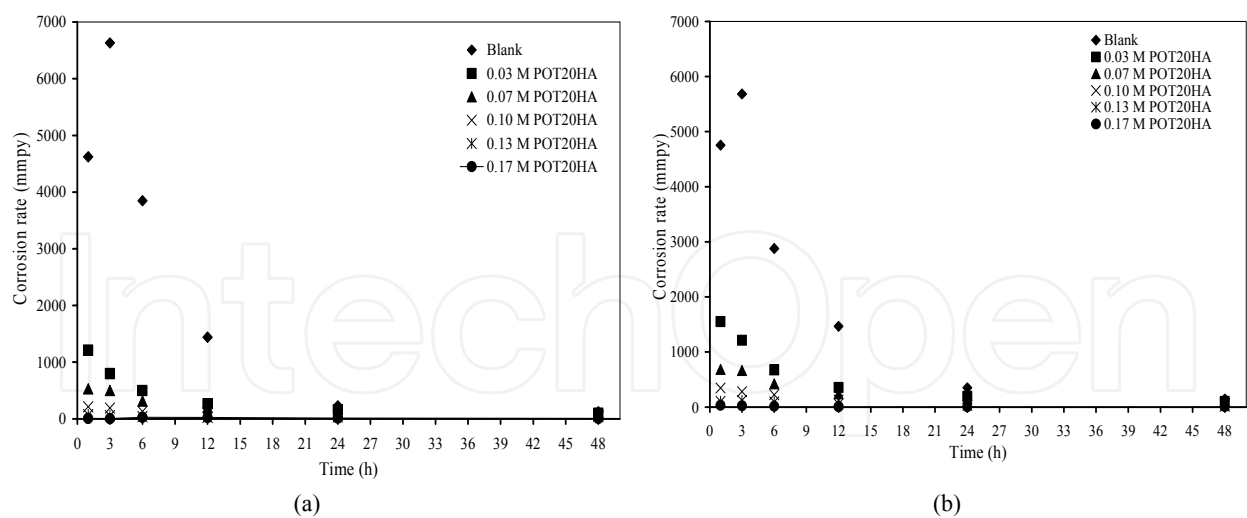


Figure 10. Corrosion rate of Al 6061 in 1 M HCl solution with the absence and presence of different concentrations of POT20HA at (a) 323 K and (b) 343 K

Inhibition Efficiency (%)					
Time (hour)	0.03 M POT20HA	0.07 M POT20HA	0.10 M POT20HA	0.13 M POT20HA	0.17 M POT20HA
299 K					
1	96	96	97	97	99
3	99	99	99	99	100
6	98	98	99	99	100
12	96	98	98	99	100
24	92	96	98	98	100
48	90	95	96	96	100
323 K					
1	74	89	95	98	100
3	88	92	97	99	100
6	87	92	97	99	99
12	82	86	92	98	98
24	32	45	70	85	95
48	21	38	50	69	92
343 K					
1	67	86	93	98	99
3	79	88	95	98	100
6	77	85	92	97	100
12	76	84	91	96	99
24	44	56	72	91	98
48	30	36	73	90	93

Table 11. Inhibition efficiency (%) of different concentrations of POT20HA at 299, 323 and 343 K from weight loss test

5.4.2. Potentiodynamic polarization study

Table 12 shows the electrochemical parameter of Al 6061 immersed in 1 M HCl in the presence and absence of different concentrations of POT20HA and temperatures. At all temperatures under study, an increase in concentration of POT20HA has reduced the corrosion potential (E_{corr}), corrosion current (i_{corr}) and the corrosion rate (CR); thus, increasing the polarization resistance (R_p). With 0.17 M POT20HA, the R_p increased remarkably as compared to those of the lower concentrations. The R_p is associated with the resistance action of POT20HA towards corrosion reaction. Accordingly, the 0.17 M POT20HA had shown the highest IE as compared to those of the lower concentrations at 299, 323 and 343 K. Furthermore, an addition of inhibitor to the corrosive solution had changed the value of the anodic and cathodic Tafel slopes, β_a and β_c respectively, as compared to those values in the absence of inhibitor. Thus, it shows that the inhibitor controls both the cathodic and anodic corrosion reactions.

It is observed that the E_{corr} of 0.03 M POT20HA shifted slightly to the left while those of the higher concentrations were shifted to the right in all of the temperatures under study. As determined from the data, E_{corr} difference between the POT20HA and the blank was less than 85 mV. Hence, the POT20HA is considered to be of the mixed type of inhibitor with predominantly anodic action, except for the 0.03 M POT20HA, which was more towards cathodic [28, 29]. This confirmed the results of β_a and β_c , which generally revealed the ability of POT20HA in protecting both the anodic and cathodic reactions of the corrosion process.

Parameter	E_{corr} (mV)	i_{corr} (mA/cm ²)	R_p (ohm.cm ²)	β_a (mV)	β_c (mV)	Corrosion rate (mm/y)	IE (%)
Concentration of POT20HA				299 K			
Blank	-759	33.504	5.65	922.9	-1209	375.20	-
0.03 M	-779	0.639	14.56	131.4	-197	7.16	98
0.07 M	-784	0.417	15.79	84.8	-170	4.67	99
0.10 M	-750	0.394	31.20	159.8	-303	4.41	99
0.13 M	-756	0.158	38.56	90.4	-272	1.77	100
0.17 M	-722	0.020	792.44	37.0	-554	0.219	100
				323 K			
Blank	-806	37.823	2.54	571.7	-715	423.600	-
0.03 M	-809	5.000	5.33	110	-287	61.280	86
0.07 M	-775	4.464	40.03	336.4	-405	14.760	97
0.10 M	-761	0.673	43.69	229.9	-287	6.781	98
0.13 M	-754	0.775	129.89	308.1	-369	7.812	98
0.17 M	-736	0.006	1530	74.8	-959	0.006	100

343 K							
Blank	-831	30.957	1.98	347.2	-453	346.700	-
0.03 M	-849	3.945	14.64	193.2	-342	44.180	87
0.07 M	-809	2.733	29.21	553.8	-475	30.600	91
0.10 M	-803	1.245	20.53	101.3	-262	13.940	96
0.13 M	-800	1.270	64.68	4.3	-452	14.220	96
0.17 M	-740	0.493	774.20	321.7	-31	4.966	99

Table 12. Polarization parameters and IE of different concentrations of POT20HA at 299, 323 and 343 K from polarization test

5.4.3. Electrochemical Impedance Spectroscopy (EIS) study

The general shape of the curve was almost similar for all concentrations of POT20HA, indicating that almost no change in the corrosion mechanism occurred when concentrations were varied [30]. Adding and increasing of POT20HA increased the capacitive semicircle loop diameter which indicated the increase in the IE (Figure 11 and 12). Furthermore, the 0.03 and 0.07 M POT20HA had shown almost similar capacitive values as shown in Figure 12 (a).

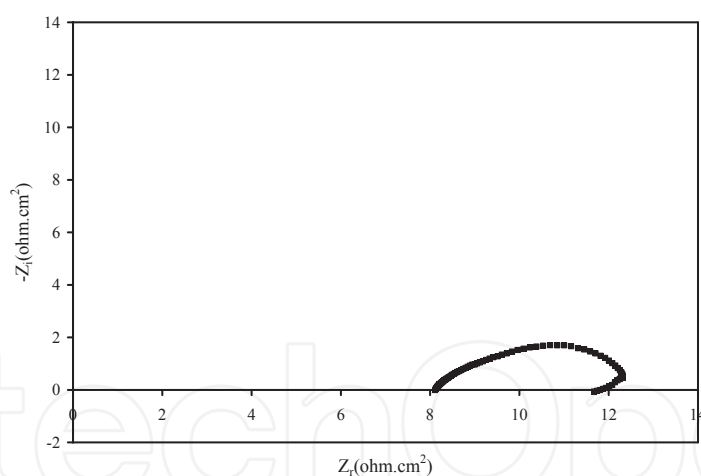


Figure 11. Electrochemical impedance plot of Al 6061 at 299 K in blank 1 M HCl solution

The impedance of Al 6061 in 1 M HCl solution with different concentrations of POT20HA at 323 K (Figure 13) was almost similar to that of the 299 K especially in the blank, 0.03, 0.07, 0.10 and 0.13 M POT20HA solution. The 0.03 and 0.07 M POT20HA had shown almost similar capacitive values; a similar behaviour was found at 299 K. Nonetheless, the impedance behaviour of 0.17 M POT20HA was rather different than those of the lower concentrations and the 0.17 M at 299 K. There was no inductance loop observed at the low frequency, which indicated the absence of passive film dissolution.

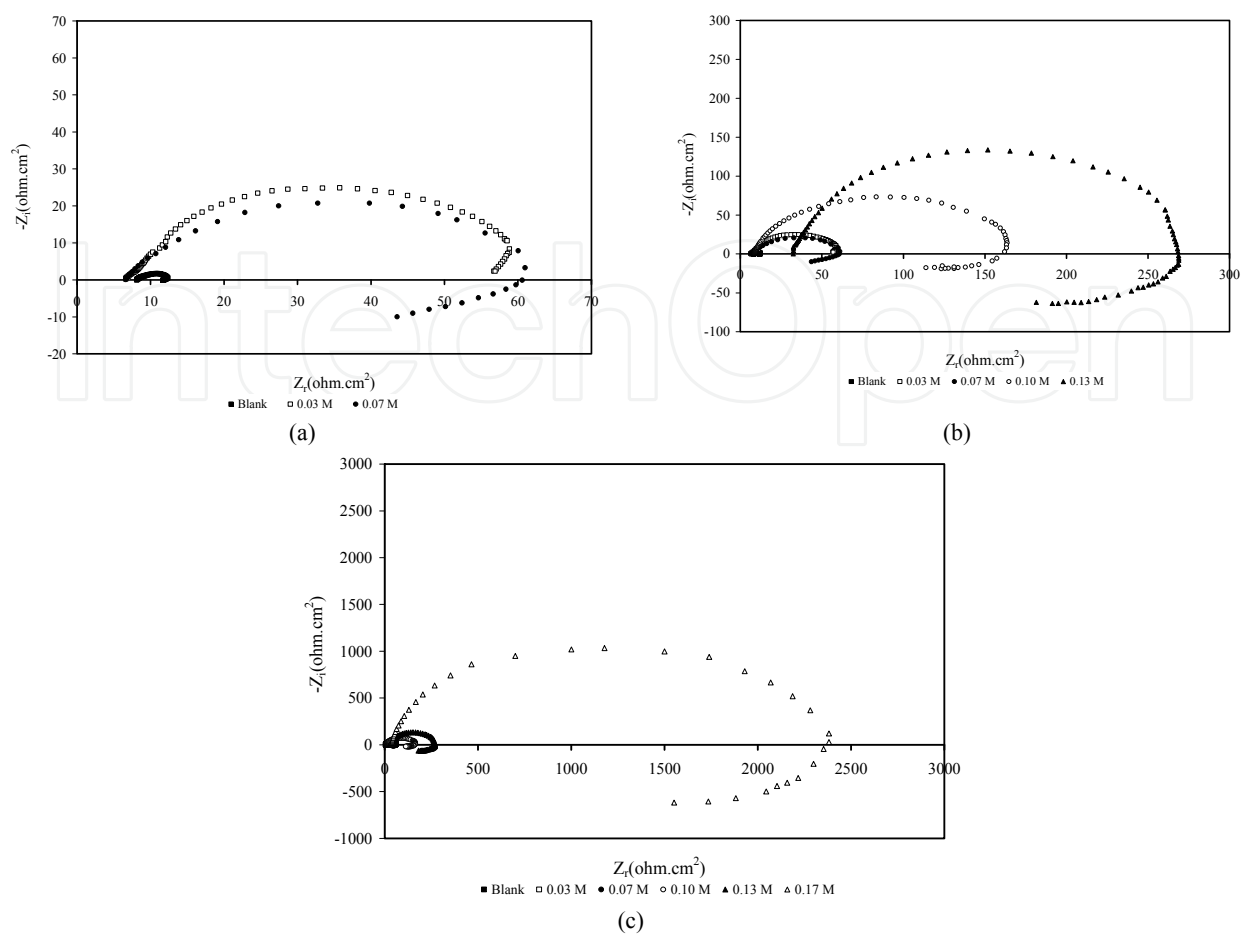


Figure 12. Electrochemical impedance plot of Al 6061 in 1 M HCl solution at 299 K zooming to (a) 0.03 and 0.07 M POT20HA and (b) 0.10 and 0.13 M POT20HA Electrochemical impedance plot of Al 6061 at 299 K in 1 M HCl solution with 0.17 M POT20HA

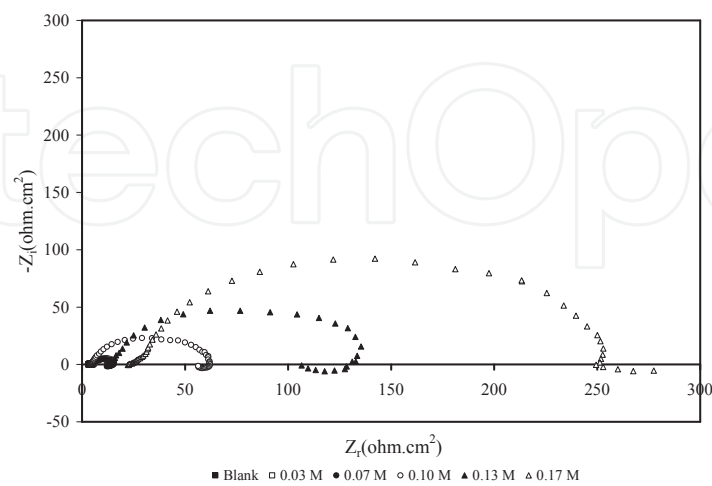


Figure 13. Electrochemical impedance plot of Al 6061 in 1 M HCl solution at 323 K at different concentration of POT20HA

The impedance of Al 6061 in 1 M HCl solution with different concentrations of POT20HA at 343 K was almost similar to those of the lower temperatures under study. The presence of inhibitor had increased the capacitive value. However, the 0.17 M POT20HA had shown different impedance behaviour than those of the lower temperatures. There was no inductance loop obtained at the low frequency and the formation of capacitive loop was not well defined as shown in Figure 14. Similar type of curve was observed by Sherif & Park and Mabroure et al. [31, 32], the significant increase in the loop size and the absence of inductance loop as compared to those of the lower concentrations of POT20HA solution indicate that the 0.17 M POT20HA had better inhibitive behaviour with no dissolution of passive film.

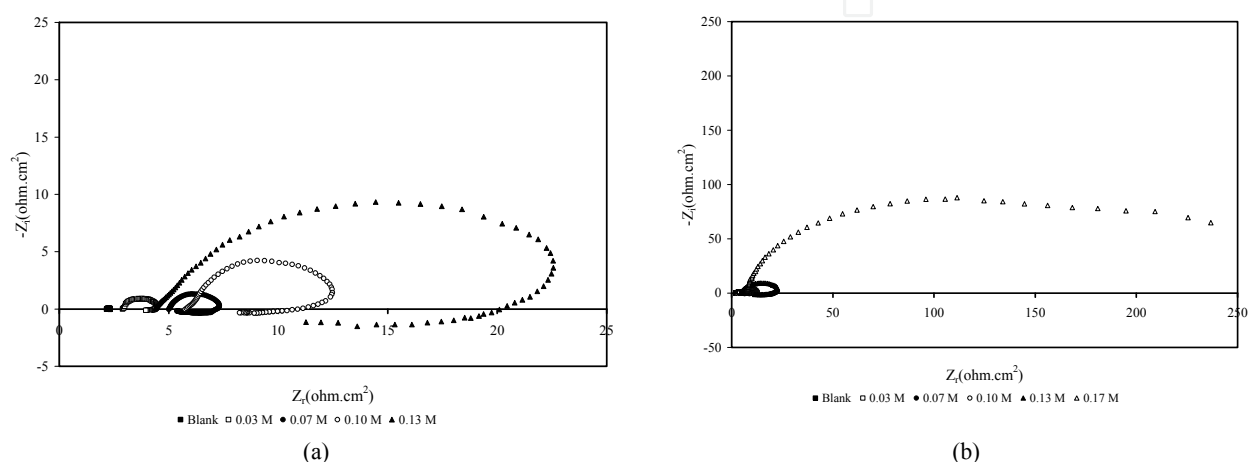


Figure 14. Electrochemical impedance plot of Al 6061 in 1 M HCl solution at 343 K at different concentration of POT20HA

Finally, results from the corrosion tests revealed the inhibition behaviour of the POT20HA towards Al 6061 at different temperatures and concentrations. The weight loss (WL) test showed that IE increased with increasing concentration but decreased with increasing of immersion time and temperature. However, the IE of the 0.17 M POT20HA remained high even after 48 hours of immersion time. The potentiodynamic polarization (PP) test revealed that the POT20HA acted as a mixed type of inhibitor which was capable in inhibiting the anodic and cathodic sides of corrosion process. Consequently, EIS results showed the ability of POT20HA in forming a protective passive film on Al 6061 surface. The thickness of the passive film increased with increasing concentration but decreased with increasing temperature. On the other hand, dissolution of the passive film occurred at elevated temperature and insufficient levels of POT20HA, causing the Al 6061 to eventually dissolve. EIS confirmed that a stable passive film was formed by 0.17 M POT20HA.

5.5. Surface corrosion analysis

SEM micrograph images, as shown in Figure 15, 16 and 17, revealed the effect of different concentrations of POT20HA on the Al 6061 after 3 hours of immersion time in 1 M HCl solution at 299 K. Morphology of the Al 6061 in 0.03 M POT20HA was almost similar to that of in the

blank solution as shown in Figure 15 and 16(a). Homogeneous corroded area throughout the surface sample showed that the corrosive solution had attacked the entire grain boundaries of the Al 6061 surface. Further increase in the concentration from 0.03 M to 0.07, 0.10 and 0.13 M showed a reduction in the surface attack as illustrated in Figure 16(b), 17(a) and 17(b), respectively. However, some of the surface was unattacked (grey area), while some intergranular corrosion was observed propagating along the grain boundaries of the Al 6061 surface. Length of the propagating intergranular corrosion reduced with the increase of concentration as clearly observed in 0.07 M and 0.13 M. Further increase in the concentration to 0.17 M showed only the presence of minor pitting corrosion as observed in Figures 18(a) and 18(b) which, revealed one of the pitting corrosion on the Al 6061 surface (at point A). The increase in concentration of POT20HA from 0.03 to 0.17 M had changed the corrosion pattern from general to intergranular and finally to pitting corrosion. Similar corrosion pattern were observed at 323 and 343 K.

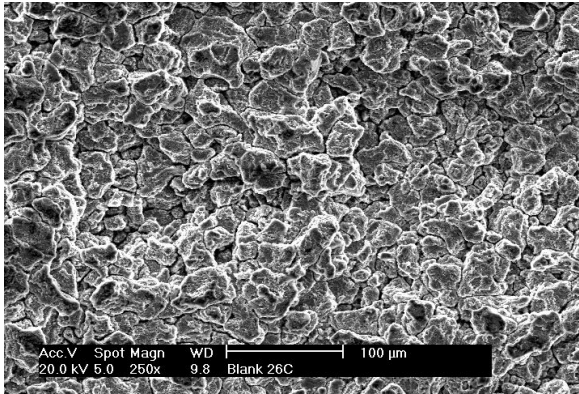


Figure 15. SEM micrograph image of the Al 6061 surface after 3 hours of immersion in blank 1 M HCl solution at 299 K

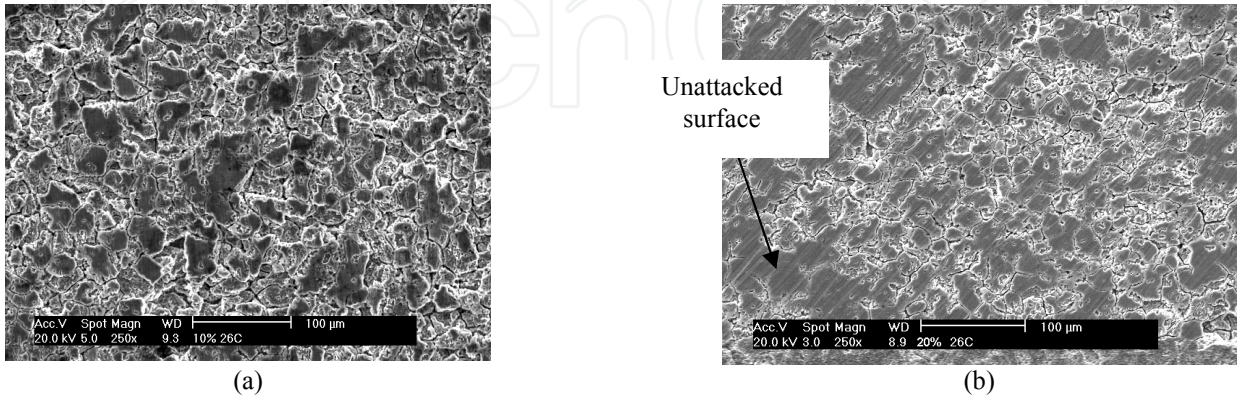


Figure 16. SEM micrograph images of the Al 6061 surface after 3 hours of immersion in 1 M HCl solution with different concentrations of POT20HA at 299 K (a) 0.03 M and (b) 0.07 M

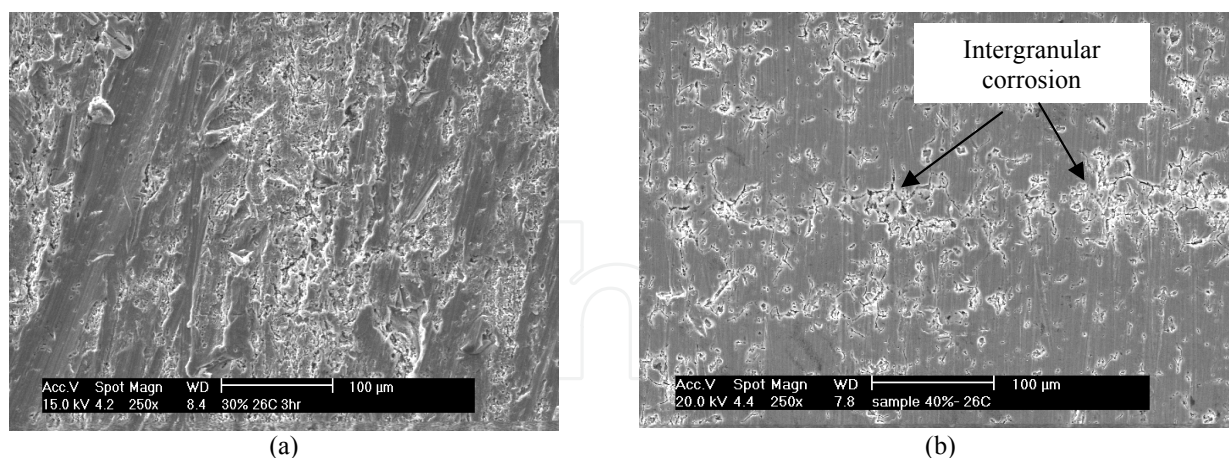


Figure 17. SEM micrograph images of the Al 6061 surface after 3 hours of immersion in 1 M HCl solution with different concentrations of POT20HA at 299 K (a) 0.10 M and (b) 0.13 M

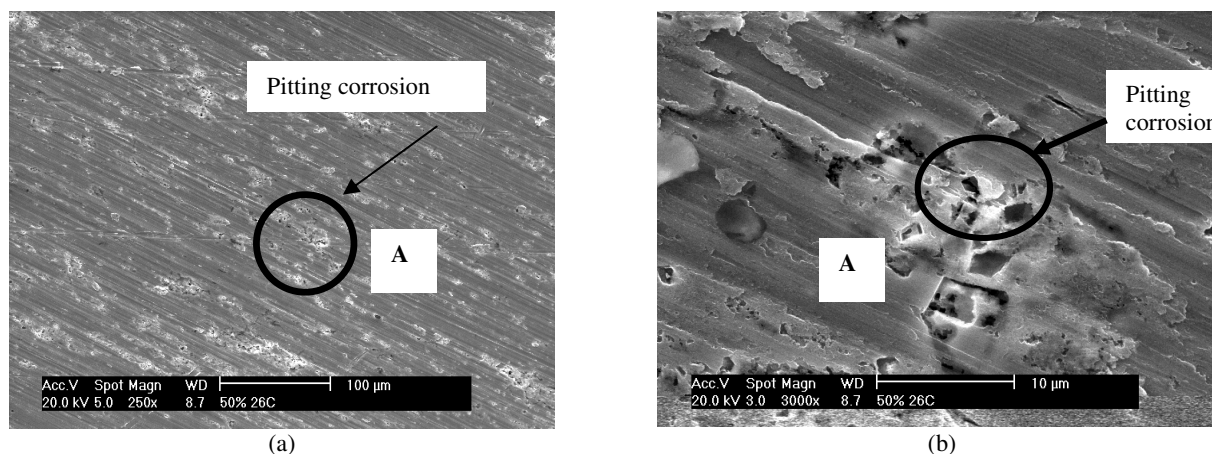


Figure 18. SEM micrograph images of (a) the Al 6061 surface after 3 hours of immersion in 1 M HCl solution with 0.17 M POT20HA at 299 K and (b) enlargement of point A

The SEM observation confirmed the results of WL, PP and EIS tests. The 0.17 M POT20HA solution showed the formation of minor pitting corrosion in all temperatures under study, thus, revealing the ability of this concentration in protecting the Al 6061 surface at these temperatures. At lower concentrations, Cl^- ions could penetrate the Al 6061 surface due to the incomplete surface coverage by the inhibitor. The penetration leads to the formation of pitting corrosion. The lower the concentration of the inhibitor, the more surface area were exposed to the Cl^- ions, hence more pitting corrosion formed which lead to the formation of intergranular and finally general corrosion. The increase of temperature would increase the activation energy of the Cl^- ions, hence increased the aggressiveness of corrosion. On the other hand, an increase in the immersion time will increase the contact between the Cl^- ions and the Al 6061 surface, thus promoting the corrosion process. However, with the 0.17 M POT20HA solution, the

aggressiveness of the corrosion process due to the temperature and immersion time can be eliminated.

5.6. Adsorption isotherm relationship

The correlation between the concentration of POT20HA (C) and surface coverage (θ) was determined by fitting the experimental data on a suitable adsorption isotherm, such as Frumkin, Temkin and Langmuir relationships. The adsorption isotherm relationships were expressed by the following equations;

$$\text{Frumkin relationship} \quad \ln\left(\frac{\theta}{C(1-\theta)}\right) = \ln K + 2a\theta \quad (5)$$

$$\text{Temkin relationship} \quad \theta = \left(\frac{1}{f}\right) \ln(KC) \quad (6)$$

$$\text{Langmuir relationship} \quad \frac{C}{\theta} = \frac{1}{K} + C \quad (7)$$

Table 13 shows the correlation coefficient (R^2) values of the experimental data (weight loss measurement) according to the respective adsorption isotherm relationship at different immersion time. The R^2 values indicated that the experimental data were in agreement with the Langmuir relationship at all temperatures under study. This condition shows that POT20HA has formed monolayer film that was attached to the Al 6061 surface without lateral interaction between the adsorbed inhibitor. However, at the 323 and 343 K, the data for the immersion time above 24 hours would fit the Temkin relationship. According to the Temkin relationship, the f values at this condition are positive. The attraction between Al 6061 and the adsorbed inhibitor is as explained by Noor [8]. The experimental data did not fit the Frumkin relationship. This finding reveals the transition from Langmuir to Temkin isotherm relationship, hence, shows that the adsorption behaviour of an inhibitor is strongly influenced by the temperature.

The inhibition adsorption of POT20HA on Al 6061 surface was determined by the standard free energy of adsorption (ΔG_{ads}^0). The ΔG_{ads}^0 value was calculated using the determined K value from the Langmuir relationship and expressed in the following equation;

$$\ln K = \ln \frac{1}{55.5} - \frac{\Delta G_{ads}^0}{RT} \quad (8)$$

Figure 19 shows the ΔG_{ads}^0 values from WL (1h), PP and EIS at different temperatures according to the Langmuir relationship. The three tests showed almost similar values of ΔG_{ads}^0 , which

Relationship	Temperature(K)	1h	6 h	24 h	48h
Langmuir	299	0.9996	0.9999	0.9999	0.9993
	323	0.9997	0.9994	0.7747	0.4303
	343	0.9995	0.9980	0.9074	0.2831
Temkin	299	0.6359	0.8980	0.9848	0.9606
	323	0.9796	0.9616	0.9220	0.8827
	343	0.9843	0.9841	0.9113	0.8447
Frumkin	299	0.0029	0.1376	0.4069	0.2582
	323	0.5352	0.6209	0.7965	0.9252
	343	0.6430	0.7965	0.9097	0.8032

Table 13. The correlation coefficient (R^2) of the experimental data from different adsorption isotherm relationships

ranged from -22 to -26 kJ/mol. These values indicated physical adsorption on the transfer of unit mole of the inhibitor from solution onto the metal surface [33]. The negative sign of the free energy of adsorption indicated the adsorption of the inhibitor at the metal surface was a spontaneous process [34]. For WL and PP, an increase of temperature from 299 K to 323 K has increased the $\Delta G_{\text{ads}}^{\circ}$ values (less negative). However further increase in the temperature to 343 K has slightly decreased (more negative) the value of $\Delta G_{\text{ads}}^{\circ}$. On the other hand, the opposite trend of the $\Delta G_{\text{ads}}^{\circ}$ values on the EIS was observed as compared to those of the WL and PP. This finding could be due to the measurement technique that was used in the EIS. Therefore, the $\Delta G_{\text{ads}}^{\circ}$ values from the EIS are not involved in the following discussion.

Similar behaviour of $\Delta G_{\text{ads}}^{\circ}$ had been observed by Noor [8] where 2 M HCl solution in the presence of inhibitor at various temperatures were studied. The increase in $\Delta G_{\text{ads}}^{\circ}$ with increasing temperature indicates the occurrence of exothermic process at which adsorption is unfavourable which cause desorption of inhibitor from the Al 6061 surface. On the other hand, the decrease in $\Delta G_{\text{ads}}^{\circ}$ value with increasing temperature indicates the occurrence of endothermic process which promotes adsorption of the inhibitor on the Al 6061 surface. When both conditions are observed within the temperature range under study it shows the occurrence of both the exothermic and endothermic adsorption processes.

5.7. Inhibition mechanism

Since the POT20HA was in the form of dilute emulsion, the adsorption mechanism of the inhibitor on the Al 6061 surface in 1 M HCl was determined through an emulsion analysis. As previously mentioned, POT20HA existed as spherical micelles with particle size ranging from 0.04 to 300 μm . The pH of emulsion was 12.5 which indicated that the micelles were negatively charge [35], thus are capable in forming electrostatic bonding or being physically adsorbed onto the positively charged Al 6061 surface. The pH of the emulsion without the presence of

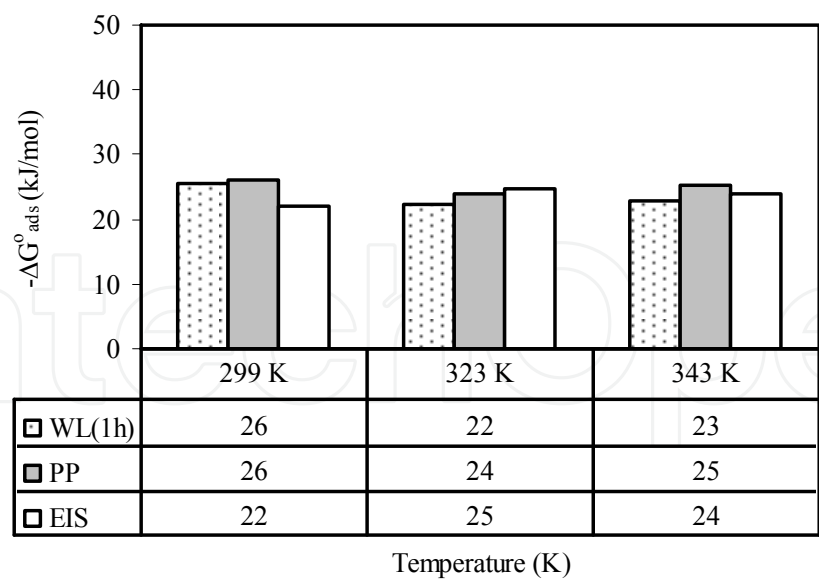


Figure 19. The $\Delta G^{\circ}_{\text{ads}}$ values of POT20HA from different corrosion tests and temperatures

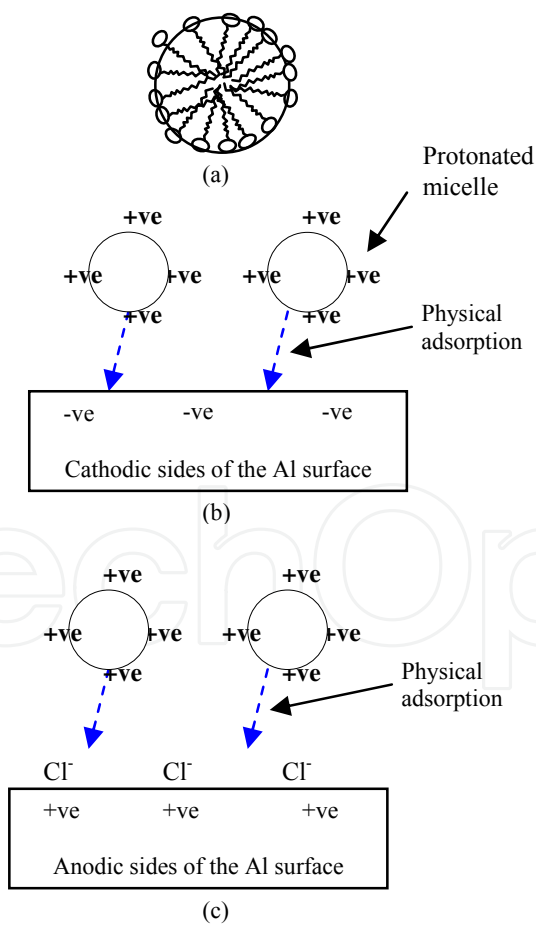


Figure 20. Adsorption of POT20HA in 1 M HCl solution; (a) spherical micelle, (b) the cathodic sides of the Al surface, and (c) the anodic sides of

DETA was about 7; therefore, it was shown that the increase in the basicity of the emulsion was due to the presence of DETA. Results showed that the inhibition was due to the presence of an amide compound (Figure 20).

The PP test had revealed that POT20HA acts as a mixed type of inhibitor which controls both the anodic and cathodic sides of corrosion reaction. Consequently, adsorption isotherm had shown that POT20HA was adsorbed on the Al surface through physical adsorption via weak van der Waal forces. In 1 M HCl solution, POT20HA which was in the form of micelles were expected to be fully protonated [36]. The carbonyl functional group of the amide family of POT20HA was expected to be protonated by the HCl solution and acted as cationic species. Thus, the protonated micelles adsorbed on the cathodic sides of the corroding surface and blocked the H₂ evolution. Figure 20(a) shows the schematic illustration of the spherical micelles, while Figure 20(b) illustrates the attachment of protonated micelles on the cathodic sides of the Al surface. Subsequently, the protonated micelles were expected to be adsorbed onto the anodic sides of the Al surface by means of electrostatic interaction. The electrostatic interaction was formed due to the presence of Cl⁻ ions in the 1 M HCl solution which were likely to be adsorbed onto the anodic sides of the Al surface and form negatively charged surface which then promoted the adsorption of the protonated micelles. This phenomenon is illustrated schematically by Figure 20(c). Hence, the presence of POT20HA in the corrosion system of Al in 1 M HCl had controlled the dissolution of Al as well as the evolution of H₂.

5.8. Performance evaluation

From the above result and discussion on the formulated corrosion inhibitor, the POT20HA would be able to protect the Al 6061 surface through physical adsorption. Hence, assumption can be made that the POT20HA is capable to work as an anticorrosion in car radiator, in which the temperature is at 88±2°C. In responding to this assumption, POT20HA was used as anticorrosion in a simulated condition of car radiator according to JIS K 2234.

The JIS K 2234 specification was taken as the reference in evaluating the performance of the PO anticorrosion-coolant in the circulation test. Table 14 shows the JIS K 2234 specification and changes of pH, mass of Al, Cu and Fe after the circulation test. In the test, the Al, Cu and Fe were immersed in a solution containing 30% (v/v) of PO anticorrosion-coolant and the balance “adjusting” water at 88±2°C for 1000±2 hours at a circulation rate of 1.5 liter/min. The result showed that the POT20HA had successfully protected the Cu, Fe and Al from corrosion within the JIS K 2234 specification for the circulation test.

JIS K 2234 specification		After the circulation test
Change of mass (mg/cm ²)	Al	±0.60
	Cu	±0.30
	Fe	±0.30
Initial pH		7 to 11
Final pH		10.40
		9.43

Table 14. Mass and pH changes after circulation test

5.9. Physical properties of PO anticorrosion-coolant

Table 15 shows the physical properties of both the PO and the commercial anticorrosion-coolants. The density and boiling points of these anticorrosion-coolants were within the acceptable range. The boiling point of PO anticorrosion-coolant was significantly much higher than those of the commercial anticorrosion-coolant and the specified values in JIS K 2234. However, the freezing point of the PO anticorrosion-coolant was slightly higher than the specified value.

Performance of the formulated PO antirust-coolant followed the specification of the JIS K 2234 and is almost similar to the well known commercial product. Furthermore, PO showed better boiling point than the commercial product, even though the freezing point was slightly lower. Therefore, the formulated PO antirust-coolant was an excellent anti-boil, anticorrosion and significant enough as anti-freeze which can be used throughout the year, especially in tropical and temperate countries.

Physical Properties	JIS K 2234	PO	Commercial
Density	1.112 (min)	1.239	1.12
Boiling Point	152°C(min)	230°C	192°C
Freezing point (50%(v/v) anticorrosion-coolant)	-34°C(max)	-26°C	-36.5°C

Table 15. The physical properties of the anticorrosion-coolant

6. Conclusions

The formulated palm olein inhibitor (POT20HA) was an amide compound which is partially soluble in water. The temperature of (50°C) 323 K and pH 7 were found to be the suitable condition for formulation preparation. The suitable emulsifier, stabilizing agent and enhancing agent were Tween 20, hexane and DETA, respectively.

The weight loss study showed that the IE was found to be concentration dependent. However the IE is inversely proportional to the immersion time and temperature. The potentiodynamic polarization study showed that the POT20HA was a mixed type of inhibitor. The electrochemical impedance spectroscopy results indicated the ability of POT20HA in forming protective passive film on Al 6061 surface. The thickness of passive film increased together with increasing concentration of POT20HA but decreased with increasing temperature. SEM observation showed a smooth and homogeneous inhibited Al 6061 surface with 0.17M POT20HA.

The Langmuir isotherm relationship fitted the data of all temperatures and immersion times under study. The ΔG_{ads}^0 and E_a values for all concentrations and temperatures under study

confirmed that the POT20HA was adsorbed on the Al surface through physical adsorption. Adsorption mechanism study had shown that the protonated POT20HA micelles in 1 M HCl was adsorbed onto the cathodic sides of the corroding surface and blocked the H₂ evolution. Subsequently, the protonated micelles of POT20HA were adsorbed onto the anodic sides of the Al surface by means of electrostatic interaction of the Cl⁻ ions.

The performance tests had shown that POT20HA had the ability to function as an anticorrosion material when mixed with glycerin in Al car radiator. Performance of the formulated PO anticorrosion-coolant fulfilled the specification of the JIS K 2234 and matched the standard of a well known commercial product.

Acknowledgements

The Ministry of Education of Malaysia is acknowledged for providing Fundamental Research Grant Scheme (FRGS) for this work. A special gratitude also goes to the Research Management Institute (RMI) of Universiti Teknologi MARA, Malaysia for the continuous supports. Special thanks to the Dean of Faculty of Chemical Engineering, Universiti Teknologi MARA, Malaysia for the support and encouragement. Finally, appreciations also go to those who are directly and indirectly involved in this work.

Author details

Junaidah Jai*

Address all correspondence to: junejai@salam.uitm.edu.my

Faculty of Chemical Engineering, University of Technology MARA, Shah Alam, Malaysia

References

- [1] Maayta A, Al-Rawashdeh N. Inhibition of acidic corrosion of pure aluminum by some organic compounds. *Corrosion Science*. 2004;46(5):1129-40.
- [2] El-Etre A. Inhibition of acid corrosion of carbon steel using aqueous extract of olive leaves. *Journal of Colloid and Interface Science*. 2007;314(2):578-83.
- [3] El-Etre A, Abdallah M. Natural honey as corrosion inhibitor for metals and alloys. II. C-steel in high saline water. *Corrosion Science*. 2000;42(4):731-8.
- [4] El-Etre A. Inhibition of acid corrosion of aluminum using vanillin. *Corrosion Science*. 2001;43(6):1031-9.

- [5] El-Etre A. Inhibition of aluminum corrosion using *Opuntia* extract. *Corrosion Science*. 2003;45(11):2485-95.
- [6] Orubite K, Oforka N. Inhibition of the corrosion of mild steel in hydrochloric acid solutions by the extracts of leaves of *Nypa fruticans* Wurmb. *Materials Letters*. 2004;58(11):1768-72.
- [7] El-Etre A, Abdallah M, El-Tantawy Z. Corrosion inhibition of some metals using *lawsonia* extract. *Corrosion Science*. 2005;47(2):385-95.
- [8] Noor EA. Temperature effects on the corrosion inhibition of mild steel in acidic solutions by aqueous extract of fenugreek leaves. *International Journal of Electrochemical Science*. 2007;2(12).
- [9] Ebenso E, Eddy N, Odiongenyi A. Corrosion inhibitive properties and adsorption behaviour of ethanol extract of *Piper guinensis* as a green corrosion inhibitor for mild steel in H_2SO_4 . *African Journal of Pure and Applied Chemistry*. 2008;2(11):107-15.
- [10] Bouyanzer A, Hammouti B, Majidi L. Pennyroyal oil from *Mentha pulegium* as corrosion inhibitor for steel in 1M HCl. *Materials Letters*. 2006;60(23):2840-3.
- [11] Benabdellah M, Benkaddour M, Hammouti B, Bendahhou M, Aouniti A. Inhibition of steel corrosion in 2M H_3PO_4 by artemisia oil. *Applied surface science*. 2006;252(18):6212-7.
- [12] Ouachikh O, Bouyanzer A, Bouklah M, Desjobert J-M, Costa J, Hammouti B, et al. Application of essential oil of *Artemisia herba alba* as green corrosion inhibitor for steel in 0.5 M H_2SO_4 . *Surface Review and Letters*. 2009;16(01):49-54.
- [13] Kalaiselvi P, Chellammal S, Palanichamy S, Subramanian G. *Artemisia pallens* as corrosion inhibitor for mild steel in HCl medium. *Materials Chemistry and Physics*. 2010;120(2):643-8.
- [14] Bammou L, Mihit M, Salghi R, Bouyanzer A, Al-Deyab S, Bazzi L, et al. Inhibition Effect of Natural Artemisia Oils Towards Tinplate Corrosion in HCl solution: Chemical Characterization and Electrochemical Study. *Int J Electrochem Sci*. 2011;6:1454-67.
- [15] Garai S, Garai S, Jaisankar P, Singh J, Elango A. A comprehensive study on crude methanolic extract of *Artemisia pallens* (Asteraceae) and its active component as effective corrosion inhibitors of mild steel in acid solution. *Corrosion Science*. 2012;60:193-204.
- [16] Huang J, Cang H, Liu Q, Shao J. Environment Friendly Inhibitor for Mild Steel by *Artemisia Halodendron*. *Int J Electrochem Sci*. 2013;8:8592-602.
- [17] Fouda A, Rashwan S, Abo-Mosallam H. Fennel seed extract as green corrosion inhibitor for 304 stainless steel in hydrochloric acid solutions. *Desalination and Water Treatment*. 2013 (ahead-of-print):1-12.

- [18] McMurry J. Organic Chemistry, United States of America: Thomson Learning. Inc; 2004.
- [19] Testing ASf, Staff M. Vol 03.02 2003: Astm Intl; 2003.
- [20] Fontana MG. Corrosion engineering: McGraw-Hill; 1986.
- [21] Al-Rawashdeh N, Maayta A. Cationic surfactant as corrosion inhibitor for aluminum in acidic and basic solutions. *Anti-Corrosion Methods and Materials*. 2005;52(3): 160-6.
- [22] Guzey D, Kim H, McClements DJ. Factors influencing the production of o/w emulsions stabilized by β -lactoglobulin-pectin membranes. *Food Hydrocolloids*. 2004;18(6):967-75.
- [23] Goyal P, Aswal V. Micellar structure and inter-micelle interactions in micellar solutions: Results of small angle neutron scattering studies. *CURRENT SCIENCE-BANGALORE*-. 2001;80(8):972-9.
- [24] Toff MRM. A comparison of the corrosion behaviour of zinc and zinc-5% aluminium coatings. United Kingdom: University of Sheffield; 1999.
- [25] Sharma S. A study on stress corrosion behavior of Al6061/albite composite in higher temperature acidic medium using autoclave. *Corrosion Science*. 2001;43(10):1877-89.
- [26] Branzoi V, Golgovici F, Branzoi F. Aluminium corrosion in hydrochloric acid solutions and the effect of some organic inhibitors. *Materials Chemistry and Physics*. 2003;78(1):122-31.
- [27] Khaled K, Al-Qahtani M. The inhibitive effect of some tetrazole derivatives towards Al corrosion in acid solution: Chemical, electrochemical and theoretical studies. *Materials Chemistry and Physics*. 2009;113(1):150-8.
- [28] Ferreira E, Giacomelli C, Giacomelli F, Spinelli A. Evaluation of the inhibitor effect of L-ascorbic acid on the corrosion of mild steel. *Materials Chemistry and Physics*. 2004;83(1):129-34.
- [29] Yan Y, Li W, Cai L, Hou B. Electrochemical and quantum chemical study of purines as corrosion inhibitors for mild steel in 1M HCl solution. *Electrochimica acta*. 2008;53(20):5953-60.
- [30] Rosliza R, Wan Nik W, Senin H. The effect of inhibitor on the corrosion of aluminum alloys in acidic solutions. *Materials Chemistry and Physics*. 2008;107(2):281-8.
- [31] Sherif E, Park S-M. Effects of 1, 4-naphthoquinone on aluminum corrosion in 0.50 M sodium chloride solutions. *Electrochimica acta*. 2006;51(7):1313-21.
- [32] Mabrouir J, Akssira M, Azzi M, Zertoubi M, Saib N, Messaoudi A, et al. Effect of vegetal tannin on anodic copper dissolution in chloride solutions. *Corrosion Science*. 2004;46(8):1833-47.

- [33] Cheng S, Chen S, Liu T, Chang X, Yin Y. Carboxymethylchitosan as an ecofriendly inhibitor for mild steel in 1 M HCl. *Materials Letters*. 2007;61(14):3276-80.
- [34] El-Etre A. Khillah extract as inhibitor for acid corrosion of SX 316 steel. *Applied surface science*. 2006;252(24):8521-5.
- [35] Liu Y, Guo R. pH-dependent structures and properties of casein micelles. *Biophysical chemistry*. 2008;136(2):67-73.
- [36] Singh P, Bhrara K, Singh G. Adsorption and kinetic studies of L-leucine as an inhibitor on mild steel in acidic media. *Applied surface science*. 2008;254(18):5927-35.